Study on High-Frequency Fluctuations in Tidal Current Direction

Patxi Garcia Novo[1], Yusaku Kyozuka[2]

[1]*Nagasaki Marine Industry Cluster Promotion Association*

1-43 Dejima-machi, Nagasaki 850-0862, Japan

[1]patxi@galaxy.ocn.ne.jp

[2]*Organization for Marine Science and Technology, Nagasaki University*

1-14 Bunkyo-Machi, Nagasaki 852-8521, Japan

[2]kyozuka@nagasaki-u.ac.jp

***Abstract*— Despite the great advances achieved in the last decade, tidal stream energy technology still has to advance some steps before becoming competitive in the energy market. One of the challenges to face is the understanding and prediction of currents. Although harmonic analysis has provided good results in the estimation of averaged current velocity and direction, in-situ measurements show a notable importance of shorter period flow fluctuations, such as those generated by turbulence conditions of the flow (<1 minute). The present paper provides a new approach for the estimation of turbulence related velocity direction fluctuations based on data measured by two ADV and two ADCP at four different locations in Goto Islands, Japan. Dividing data in short period groups (3 minutes for ADV data, 5 minutes for ADCP data), results show a lineal correlation between different percentiles of opening angle and turbulence intensity. Due to the capability of numerical models to estimate this second parameter, this approach opens the door to prediction of high frequency fluctuations on flow direction.**

***Keywords*— Tidal current, Turbulence, Flow direction, ADV, ADCP.**

I. Introduction

Over the last decades, big efforts have been done in the tidal stream energy field. Predictability of power production, minimum environmental impact, no land occupation and high global technically harvestable resource (≈1 TW) [1] make of this technology a promising alternative to the fossil fuels and nuclear fission based resources. Nevertheless, some stages should be overcome before commercial exploitation. One of these stages is related to a better understanding of tidal currents. Despite capability of numerical and tidal harmonics based methods have been widely proven for averaged velocity estimation, in-situ measurements have shown frequency fluctuations independent of harmonics effect. One of the phenomena causing this fluctuation is turbulence, generating variations in flow velocity and direction over time scales less than 1 minute [2], which may affect the converters behaviour and which have been considered unpredictable. To date, work regarding this kind of fluctuation involves in-situ measurement with high sampling frequency devices. However, quoting the words of Godin [3], "the study of currents is essentially a research problem and should not be considered a matter for routine data processing at the clerical or technical level".

In this regard, some researchers have recently focused on the evaluation of flow velocity fluctuations [4, 5], proposing different methods for its prediction. One of these approaches [5] is based on the separation of measured data in relatively short periods (3 minutes). For every period, a lineal correlation between peak velocity, turbulence intensity and averaged velocity was observed. Since both turbulence intensity and averaged velocity can be predicted by numerical modelling [6, 7], this approach makes peak velocity prediction by numerical methods possible.

Based on this method, the present paper aims to provide a similar empirical approach for the estimation of flow direction fluctuations due to turbulence conditions, relating opening angle between different percentile angles (99.9-0.1; 95-5; 90-10; …) with turbulence intensity. The hereby-presented method is based on data measured by two ADV and two ADCP in four different locations in Goto Islands, Nagasaki Prefecture, Japan.

II. Data Measurement

Goto archipelago (Fig. 1) is a group of around 140 islands in southwestern Japan. Within the 140 islands, five of them form four main channels between them (Tanoura Strait, Naru Strait, Takigawara Strait and Wakamatsu Strait). Water flowing from the Japan Sea to the Pacific Ocean during ebb tide, and vice versa during flood tide, generates strong tidal currents through these channels. In fact, due to its high potential, Tanoura Strait and Naru Strait have been recently proposed for testing tidal current converters by the Nagasaki Prefectural Government [8]. At this area, tide type is typically mixed and mainly semidiurnal, with M2 as the main tidal constituent [9], and maximum tidal range is close to 3 meter [10].

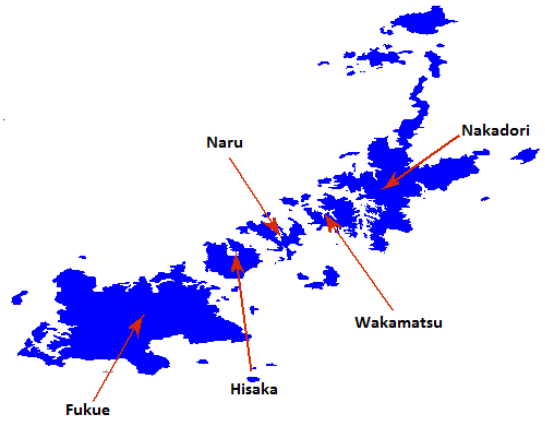

Fig. 1 Map of Goto archipelago.

The areas selected for data collection were three: Tanoura Strait, Naru Strait and Kobe Strait, a small ramification within Wakamatsu Strait. The device distribution of measuring devices is as follows: one ADV in Tanoura Strait, one ADV in Naru Strait, one ADCP in Naru Strait and one ADCP in Kobe Strait. Measuring campaigns for each of the above presented points have been widely described in previous studies [5]. Thus, in the present paper, only results concerning the main topic of this study, flow direction and turbulence intensity, are presented. It must be remarked, that all data were denoised following manufacturer recommendation [11], dropping all data for which correlation is lower than 50% in the ADCP cases and 70% in the ADV cases. Moreover, data was rotated to an N-S axis parallel distribution by a least square method in order to get a better understanding of the results.

The first ADV (P1) was installed in (32º 46' 45.2" N 128º 50' 03.1" E), operating during 8 days from November 17th in 2014. The device, marked its location in Fig. 2, was set to measure in 10-minutes cycles of 3 minutes ON and 7 minutes standby. The sampling frequency was 32 Hz, thus collecting 5760 data for every 3-minutes interval. Averaged depth for the measuring period was 26.1 m, and the device was installed at a distance of 3 meter from the bottom. Flow fluctuation for two 3-minute periods with an averaged velocity magnitude of 1.5 m/s representing flood (blue dots) and ebb (red dots) tide conditions is represented in Fig. 3. This figure clearly shows the importance of variations in terms of both magnitude and direction. Within a 3-minutes period, magnitude fluctuates between approximately 0.6 m/s to 2.3 m/s in both cases, while opening angles of 66.72° and 74.82° were found for ebb and flood tide, respectively.

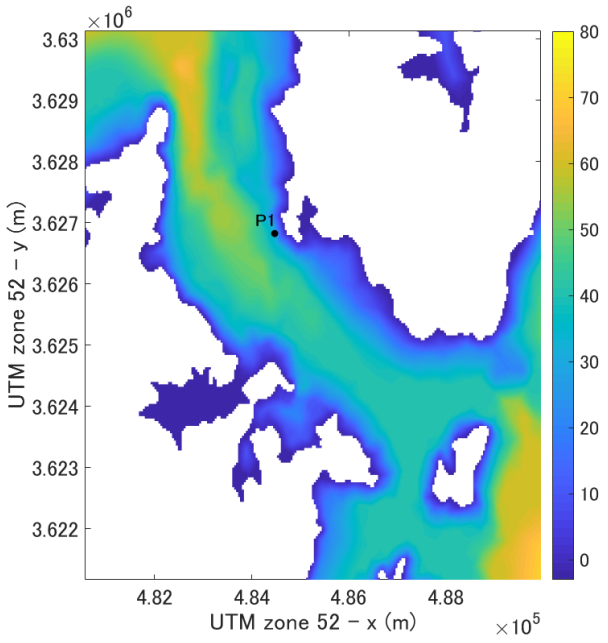

Fig. 2 Bathymetry map of Tanoura Strait.

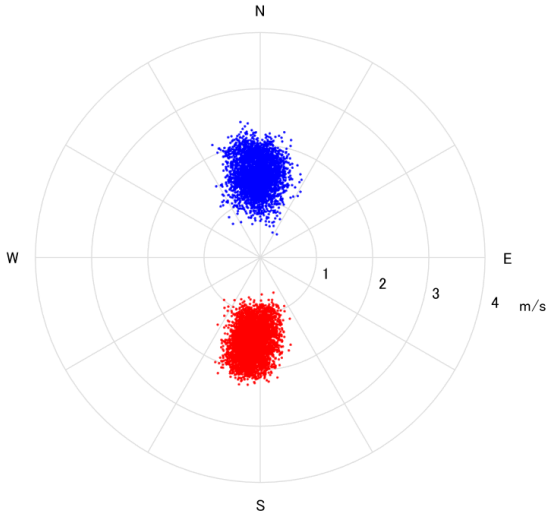

Fig. 3 Flow velocity distribution of 32Hz data for 3-minute periods for which averaged velocity magnitude is ≈1.5 m/s (red dots represent ebb tide conditions, blue dots represent flood tide conditions) in P1.

The connection between flow opening angle and turbulence appears clear in the graph in Fig. 4, which shows TI vs angle for all the 3-minute data periods for which averaged velocity is higher than 0.7 m/s, a common cut-in speed in existing commercial scale tidal current converters [12]. The great majority (shown in the red box) of represented points show a lineal correlation between both parameters, except for some outliers with very high angles (up to ≈3.6 rad). However, these exceptions are mainly due to direction fluctuations at very low velocities (<0.7 m/s), so that the effect on turbine behaviour can be considered negligible.

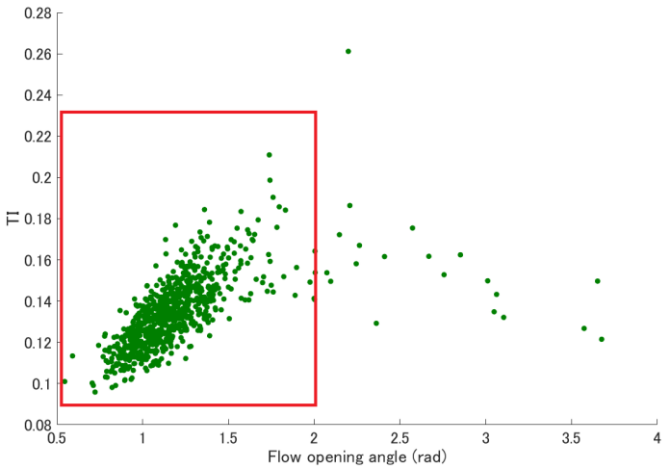

Fig. 4 Flow opening angle vs turbulence intensity (V>0.7 m/s) in P1.

During the same period in November 2014, a second ADV (P2) was operating with the same set-up in Naru Strait at (32º 49' 41.1" N 128º 58' 56.4" E). The device was also installed at three meters from the sea bottom and the averaged depth for the 8-days period was 24.6 m (see Fig. 5). Figures analogous to the presented for P1 in Tanoura Strait are built with the data measured in P2.

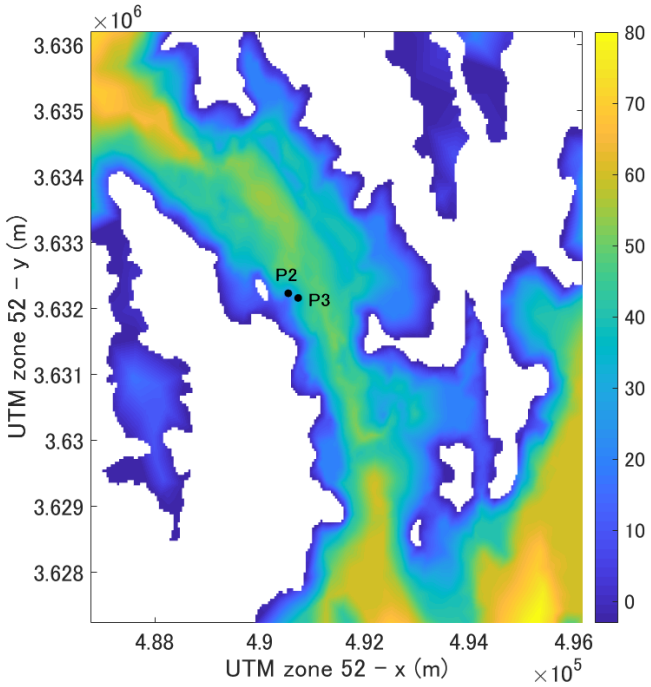

Fig. 5 Bathymetry map of Tanoura Strait

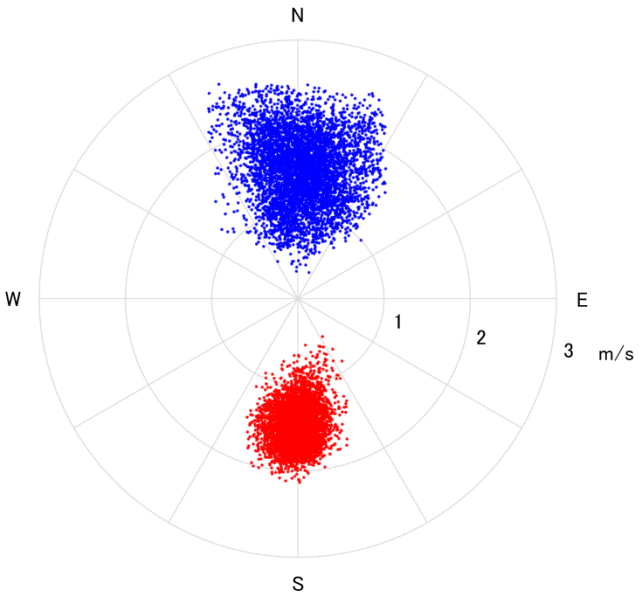

Fig. 6 Flow velocity distribution of 32Hz data for 3-minute periods for which averaged velocity magnitude is ≈1.5 m/s (red dots represent ebb tide conditions, blue dots represent flood tide conditions) in P2.

Results show a clear variation depending on tide direction. While for ebb tide results look similar to the presented for P1 in Tanoura Strait, flood tide points show a more scattered nature, both in terms of magnitude and direction. This is reflected numerically in the difference between maximum and minimum velocities (2.23 m/s for flood 3-minute representative period and 1.59 m/s for ebb tide) and in the opening angles (95.01° and 60.56°, respectively). This is due to the local geomorphologic conditions at the approaches of the measuring point, with a small underwater cape close to the ADV being the probable cause.

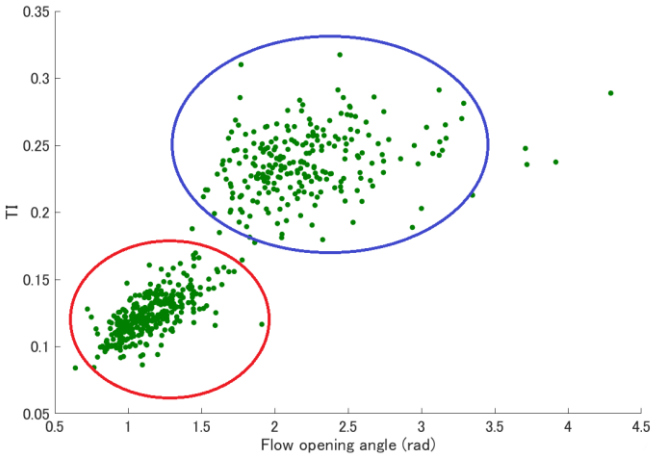

Fig. 7 Flow opening angle vs turbulence intensity (V>0.7 m/s) in P2.

As well as for P1, with the exception of some outliers with very high angles, a lineal trend appears between turbulence intensity and the opening angle. In this case, it is also remarkable the difference between flood (blue circle) and ebb

(red circle) conditions. However, the same trend is followed in both cases, which suggests that this correlation can be common to different flows and turbulent characteristics.

Also in Naru Strait, an ADCP (P3) was measuring 8 Hz data from April 14th to May 24th, 2016. The installation point was (32º 49' 38.8" N 128º 54' 03.7" E) and the averaged depth during the measuring period 35.0 m (see Fig. 5). This ADCP was set to measure in 20-minutes cycles of 5 minutes ON and 15 minutes standby. Data was collected for 22 vertical layers, each of them 1 meter width, covering approximately two-thirds of the water column. Flow fluctuation for two 5-minute periods with an averaged velocity magnitude of 1.5 m/s at a middle layer (11th layer, 12 m from the bottom) are represented in Fig. 8, which shows ebb and flood conditions at four representative vertical layers.

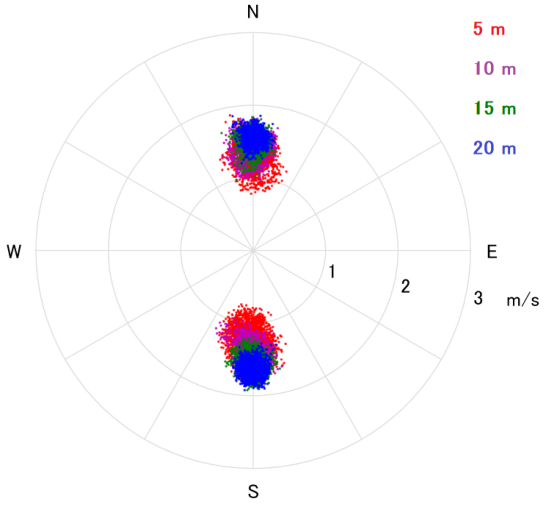

Fig. 8 Flow velocity distribution of 32Hz data for 3-minute periods for which averaged velocity magnitude is ≈1.5 m/s at layer 11 in P3.

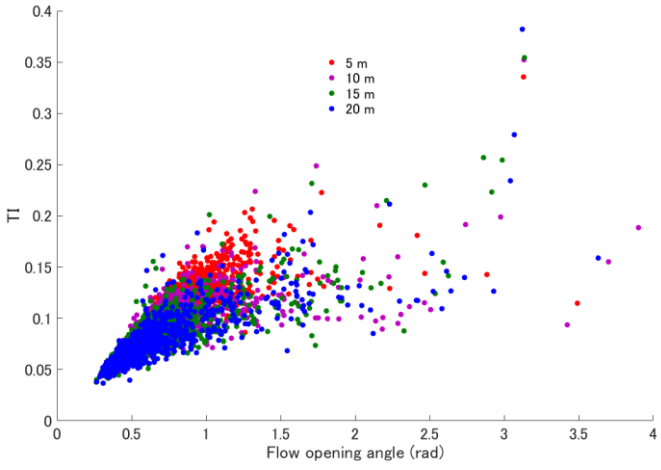

Fig. 9 Flow opening angle vs turbulence intensity (V>0.7 m/s) at different representative depths in P3.

In Fig. 8, a more scattered distribution can be observed at deeper layers both for ebb and flood conditions due to the strongest turbulence conditions resulting of bottom friction. This is also reflected in the velocity magnitude statistical ranges and opening angles (see Table 1).

TABLE I
MAGNITUDE STATISTICAL RANGE AND OPENING ANGLES AT P3

Distance to bottom (m)	Tide direction	Magnitude statistical range (m/s)	Opening angle (°)
5	flood	1.1065	41.83
	ebb	1.0623	43.91
10	flood	0.8583	31.27
	ebb	0.8523	39.47
15	flood	0.8267	27.57
	ebb	0.7280	26.88
20	flood	0.6532	20.97
	ebb	0.6432	23.70

Nevertheless, as well as for the different turbulent nature of flow for both tide directions in P2, excluding outlier points due to flow direction fluctuations at very low velocities, the trend shown in Fig. 9 between turbulence intensity and angle is very similar for the four analysed layers.

These results were corroborated with those obtained from data measured by an ADCP in Kobe Strait (P4) at (32º 52' 40.81" N 129º 01' 46.79" E) from February 27th to March 14th, in 2015 (see Fig. 10). Measuring cycles were set similarly to the ADCP in P3 (5 min ON, 15 min OFF). In this case, 36 0.5-meter layers were measured, thus covering the total water column of 18 meter. The layer closer to sea bottom was discarded due to bad quality data. Likewise, layers 29 to 36 were avoided due to unrepresentative data because of water surface interaction. As for P3, fluctuations for two 5-minute periods with an averaged velocity magnitude of 1.5 m/s at a middle layer (18th layer, 9 m from the bottom) can be observed in Fig. 11. Information shown in this figure is also summarized in Table II. In this case, due to the shallower nature of the channel only layers at 5 m, 10 m and 15 m from the bottom are described. Results obtained for flood tide are comparable to those obtained at P3, with more scattered conditions at deeper layers due to the sea bottom influence. During ebb tide, flow conditions suffer a higher impact from local geomorphologic conditions, such as the little cape some meters west of the measuring point or the division of the main stream in port and channel currents, generating more fluctuation at 10 m and 15 m from the seabed.

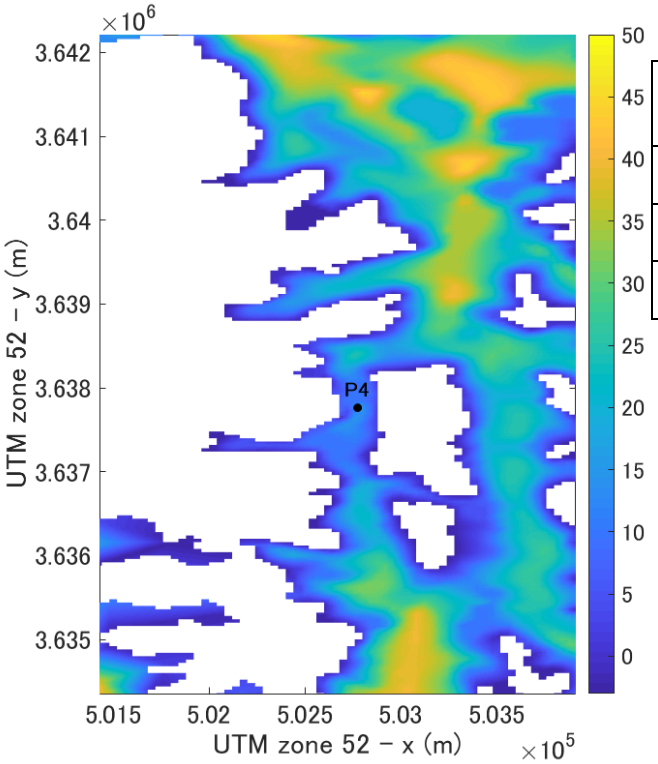

Fig. 10 Bathymetry map of Tanoura Strait

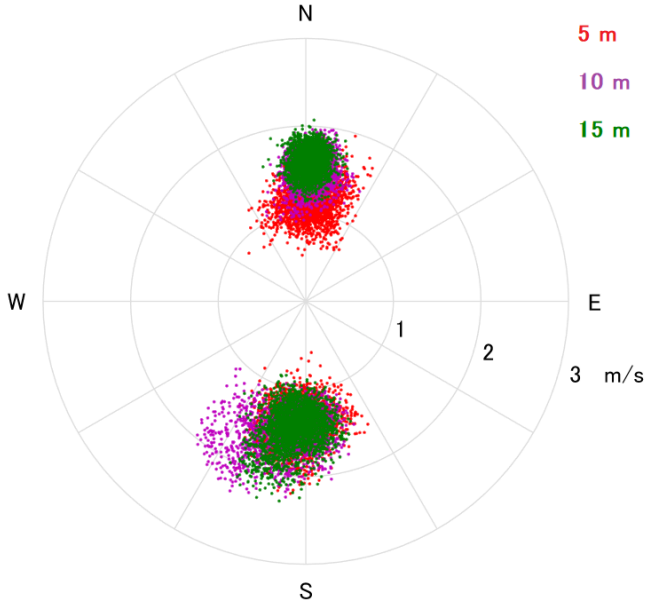

Fig. 11 Flow velocity distribution of 32Hz data for 3-minute periods for which averaged velocity magnitude is ≈1.5 m/s at layer 11 in P4.

TABLE III
MAGNITUDE STATISTICAL RANGE AND OPENING ANGLES AT P4

Distance to bottom (m)	Tide direction	Magnitude statistical range (m/s)	Opening angle (°)
5	flood	1.4410	61.10
	ebb	1.6101	49.78
10	flood	1.0511	38.23
	ebb	1.3608	68.83
15	flood	0.9237	29.35
	ebb	1.4252	52.90

Fig. 12 shows a representation of flow opening angle variation with turbulence intensity. As for P3 (Fig. 9), contrasting spatial distributions due to the different turbulence conditions were observed, with a same trend common to the three representative vertical layers.

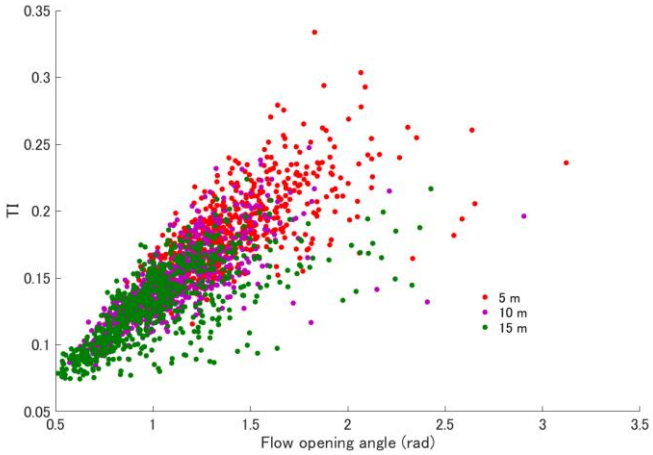

Fig. 12 Flow opening angle vs turbulence intensity (V>0.7 m/s) at different representative depths in P4.

III. ANGLE-TI CORRELATION

Analysis of the data measured at the four points shows a clear correlation between turbulence intensity and the flow opening angle for every 3-minutes or 5-minutes period (ADV or ADCP, respectively). In this section, this correlation will be parameterized. As well as for the total opening angle, other representative angles were studied in order to get a deeper understanding of fluctuations. With this aim, various percentiles were extracted for each 3-minutes or 5-minutes period (see Fig. 13). The studied angles are shown in Table III.

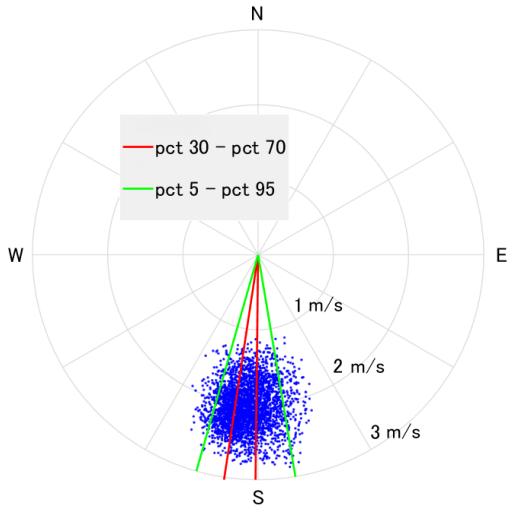

Fig. 13 3-minute current velocity direction fluctuation measured by an ADV (32 Hz).

The procedure used for each angle evaluation, adapted from a previous study focused on extreme velocities estimation [5], is described below. First, every representative angle was extracted from each 3-minutes or 5-minutes for which averaged current velocity is higher than 0.7 m/s. With these results, regression equations angle-TI were calculated separately for every vertical layer and point. After this, 5% farthest points from the regression line obtained are removed to avoid outliers and the final correlation equation is recalculated with the remaining 95%.

Finally, a prorated average line is calculated with the 52 regression equations (1 in P1, 1 in P2, 22 in P3 and 28 in P4) and their 10% prediction level. The resulting trend lines (one for each representative angle) are proposed as tools for estimation of turbulence related flow direction fluctuation. For every percentile angle, this final equation, as well as all the 52 individual equations, has the shape:

$$Ang = a \times TI + b$$

Assuming null fluctuation for a zero-turbulence flow, the final approach can be defined as:

$$Ang = a \times TI$$

It is important to emphasize that despite 5% of points are dropped, difference between preliminar and final *a* is very low, as it can be observed in the relative errors presented in Fig. 14, so that unreal results due to this previous step can be ruled out.

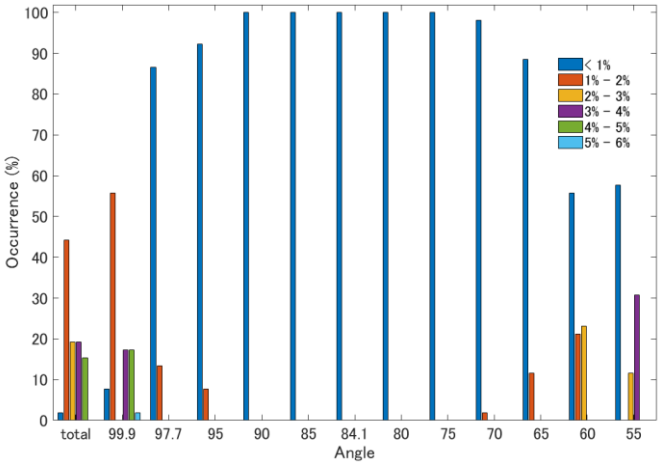

Fig. 14 Relative error between "a" calculated before and after discarding 5% farthest points for different angles.

As an example, points and trend lines resulting from discarding 5% of farthest points are shown in Fig. 15 for total angle, pct99.9-pct0.1, pct97.7-pct2.3, pct90-pct10 and pct75-pct25 in P2 in Naru Strait. Lineal trends are observed for the four cases, the slope gradually decreasing from total angle to more centred percentiles. The adaptability of lineal equations to measured data increases for central angles (pct75-pct25) since the impact of punctual data far from trend is less important than for wider angles. This is reflected also in the correlation coefficients: 0.9252, 0.9653, 0.9901, 0.9963 and 0.9946, in the same order as presented above in this paragraph. Also, as in Fig. 7, for the five represented angles two clear dot areas are differentiated for flood (right) and ebb (left) tide, with the trend line well adapted to both.

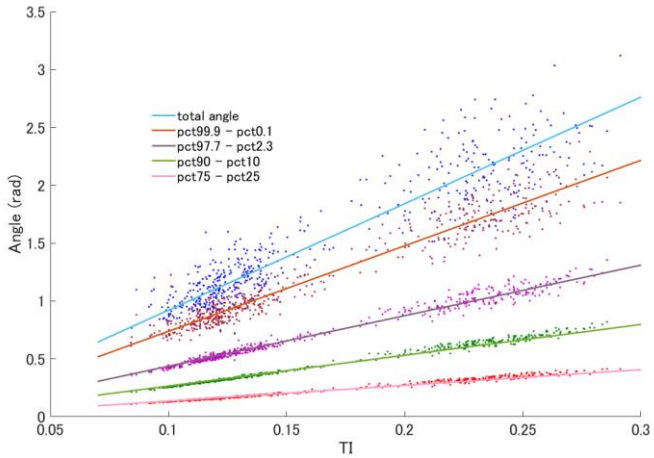

Fig. 15 Angles vs turbulence intensity at P2 (ADV Naru Strait)

Comparing results obtained at four locations and with different device setups in terms of sampling frequency, measuring cycles,… (Fig. 16), a relatively important contrast between results from ADV and ADCP is observed for the widest angles (total angles and pct99.9-pct0.1), while for more centred angles this difference decreases (pct97.7-pct2.3)

or even disappears (pct75-pct25). However, due the small amount of ADV data, conclusions cannot be extracted in this regard.

Regarding ADCP vertical layers, a direct dependence between depth and the averaged *a* parameters is not observed for any of the ADCP locations, so that its influence was not considered for this study.

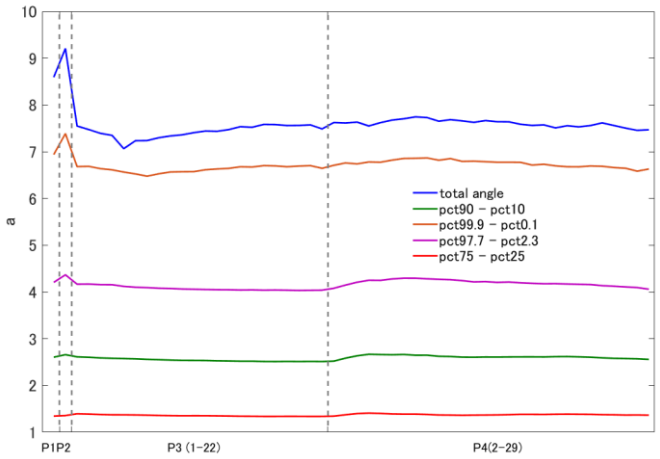

Fig. 16 "a" for the two ADV and all vertical layers of the two ADCP for different angles.

Following the same procedure mentioned above for all the points, layers and angles, the prorated *a* values presented in Table IV were obtained. These results are compared with the theoretical normal distribution in Table III and graphically in Fig. 17, for which the empirical bell is drawn assuming a symmetric distribution. Results show a distribution relatively close to the normal, with slightly higher amplitude from pct90-pct10 to pct99.9-pct0.1.

TABLE IIIII
AVERAGED, STANDARD DEVIATION AND CORRESPONDING NORMAL DISTRIBUTION FOR THE DIFFERENT ANALYSED ANGLES

Angle	Avg prorated a	Std prorated a	Normal Dist
Total	7.6247	0.3283	
99.9-0.1	6.7427	0.2199	6
97.7-2.3	4.1679	0.0623	4
95-5	3.3819	0.0470	3.29
90-10	2.6020	0.0284	2.564
85-15	2.0916	0.0160	2.072
84.1-15.9	2.0136	0.0142	2
80-20	1.6943	0.0070	1.684
75-25	1.3875	0.0091	1.35
70-30	1.1064	0.0128	1.048
65-35	0.8377	0.0152	0.77
60-40	0.5690	0.0154	0.506
55-45	0.2942	0.0129	0.252

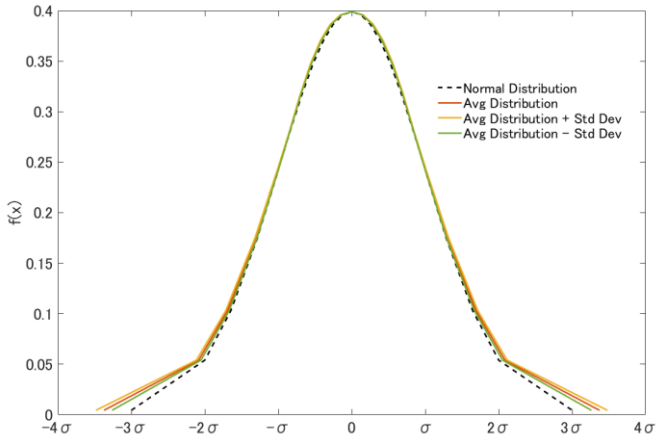

Fig. 17 Comparison of measured angles distribution with theoretical normal distribution..

IV. APPROACH EVALUATION

The obtained approaches were evaluated by comparing the angles calculated from turbulence intensity using the *a* values presented in Table III with the measured angles for every location and vertical layer (only for 3-minutes or 5-minutes data periods with averaged velocity higher than 0.7 m/s). This evaluation was done in terms of absolute errors, relative errors and prediction levels, defined as the percentage of points under a given error limit. For the error calculation, devices compass accuracy (2°) was integrated, so that for gaps lower than 2° between measured and calculated angle, errors are considered null.

Regarding total opening angle, very low averaged absolute errors are found at each of the 52 studied cases (four locations and ADCP vertical layers). The higher values were found at P2 in Naru Strait (13.16°), while for P1 and the different vertical layers in P3 and P4 the averaged absolute error is always under 7.5°. This is mainly due to the very uncommon turbulence conditions during flood tide at this location. As shown in Fig. 18, for more centered angles differences between measured and calculated are clearly reduced. For pct95-pct5, the highest averaged absolute error (again in P2) is close to 0.3°.

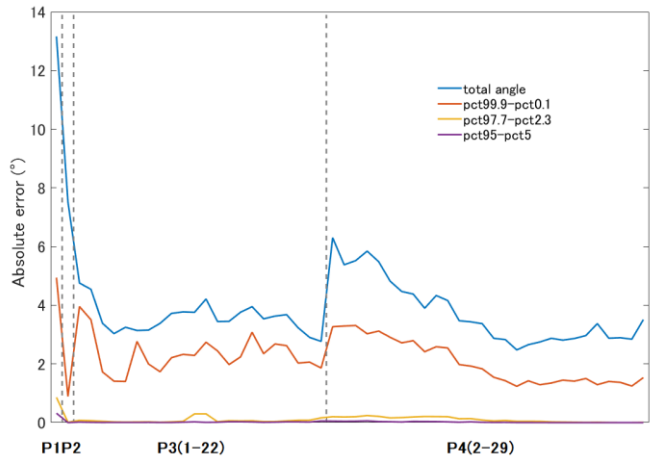

Fig. 18 Averaged absolute errors for various angles at every location and vertical layer.

Despite the relatively high averaged absolute error values for the estimation of total angle in some of the analysed locations, the validity of this approach is demonstrated by the prediction levels, defined as the percentage of cases whose estimation is within a relative error *l* around the real value. Prediction levels for *l=0.1*, *l=0.15* and *l=0.25* are presented in this paper.

Fig. 19 Prediction levels 0.1, 0.15 and 0.15 for various angles at every location and vertical layer.

Even for the worst case (again ADV in P2 in Naru Strait), for more than 73% of cases total angle can be predicted with a 10% margin of error. This percentage increases to 85% and 92% for prediction levels 0.15 and 0.25, respectively. As shown for absolute error, Fig. 19 shows better results for more centred angles. For the pct99.9-pct0.1 angle lower prediction levels are 86.1%, 90.6% and 95.0%, while for pct97.7-pct2.3 98.0%, 98.9% and 99.6%, respectively.

The good results presented below are finally corroborated by comparing graphically the data measured in P2 (ADV in Naru Strait) with the assessment made by the obtained approaches for the various angles. This comparison is represented in Fig. 20. In this figure, points representing 3-minutes period data for which averaged velocity is lower than 0.7 m/s were deleted in order to get a clearer graph.

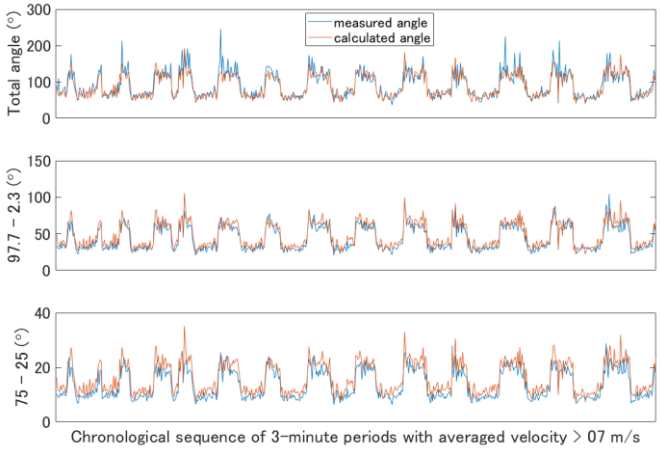

Fig. 20 Comparison of real and estimated angles in P2 (ADV in Naru Strait).

A good agreement between both lines appears, with correlation coefficients of 0.890, 0.947 and 0.935 for the total angle, pct97.7-pct2.3 and pct75-pct25, respectively. Seeing the good results for P2, where the more heterogeneous turbulence conditions and the lower prediction levels were observed, it can be expected that a good correlation will be also obtained for the other points and vertical layers, confirming the validity of the tool presented in this paper.

V. Conclusions and Future Work

Using 32 Hz data from two AVD and 8 Hz data from two ADCP measuring in four locations around Goto Islands, Japan, a new empirical method for the estimation of tidal current direction fluctuation is presented in this study. Analysing each 3-minutes or 5-minutes (for ADV and ADCP) data period, a clear direct correlation between turbulence intensity and current direction opening angles was observed. This correlation can be defined by *ANG=a x TI*. 52 spatial cases (1 for each ADV + 22 vertical layers for one ADCP + 28 vertical layers for the other ADCP) were treated separately. Their results were summarized in a common equation obtained from the *a* values for each case and the corresponding prediction levels (0.1). This procedure was done for several representative angles: total angle, angle between percentile 99.9 and percentile 0.1, between percentile 97.7 and 2.3, etc. The final results, presented in Table III, show a distribution similar to a Gauss bell with higher f(x) for σ>2.

These approaches were found capable for the estimation of turbulence related direction fluctuation at every location and vertical layer. For the 52 analysed cases, higher averaged absolute error for the total angle estimation was 13.16°, which decreases for more centered angles (0.3° for pct95-pct5). In terms of prediction level, this approach was able to estimate total angles within a margin of error of 25% for more than

92% of the 3-minutes or 5-minutes periods in all the 52 studied cases.

Future research should be focused on two directions: 1) evaluating this approach for other different locations, depths, flow characteristics and measuring devices; 2) including this approach in numerical models in order to predict tidal current direction fluctuations without the need for in-situ measurement.

ACKNOWLEDGMENT

Authors would like to thank the Ministry of Environment of Japan for the permission for publication of the data used in this study, which were obtained through the project for Promotion of Realization of Tidal Current Power Generation supported by the ministry in 2014 and 2015.

REFERENCES

[1] Carbon Trust (2011). Accelerating marine energy. "The potential for cost reduction". *Insights from the Carbon Trust Marine Energy Accelerator*. https://www.carbontrust.com/media/5675/ctc797.pdf

[2] B. L. Polagye, J. Epler, J. Thomson, "Limits to the predictability of tidal current energy", in *OCEANS 2010*. DOI 10.1109/OCEANS.2010.5664588.

[3] G. Godin, *Tides*. ANADYOMENE ed. Ottawa, 1988.

[4] S. Harding, J. Thomson, B. Polagye, M. Richmond, V. Durgesh, I. Bryden. "Extreme value analysis of tidal stream velocity perturbations". In *Proceedings of the 9th European Wave and Tidal Energy Conference*, Southampton, UK, 2011.

[5] P. Garcia-Novo, Y. Kyozuka, M. Tsuda. "Estimation of tidal peak velocity by an empirical approach" in *Proceedings of EWTEC2017*, Cork, Ireland, 2017.

[6] Carballo R, Iglesias G, Castro A. "Numerical model evaluation of tidal stream energy resources in the Ria de Muros (NW Spain). *Renewable Energy*, 34, 1517-1524, 2009.

[7] M. Togneri, M. Lewis, S. P. Neill, I. Masters. "Comparison of ADCP observations and 3D model simulations of turbulence at a tidal energy site. *Renewable Energy*, 2017

[8] Marine Industry Development Office, Industry & Labor Department, Nagasaki Prefectural Government. "Invitation to Join Nagasaki Prefecture's Efforts to Build Up Marine Renewable Energy Industry". https://www.pref.nagasaki.jp/shared/uploads/2015/04/1428657512.pdf

[9] S. Waldman, S. Yamaguchim R. O'Hara Murray, D. Woolf. "Tidal resource and interactions between multiple channels in the Goto Islands, Japan". *International Journal of Marine Energy 19*, pp 332-344. 2017

[10] Japan Meteorologic Agency. www.jma.go.jp/jma/index.html

[11] P. J. Rusello. "A practical primer for pulse coherent instruments". Nortek technical note TN-027. NortekUSA.

[12] V. Ramos, R. Carballo, M. Alvarez, M. Sanchez, G. Iglesias. "A port towards energy self-sufficiency using tidal stream power. *Energy 71*, pp. 432-444. 2014.